Evaluación de la partición de lluvia en dos especies arbóreas con *Arduino*

Evaluation of rain partitioning in two tree species with Arduino

Daniel García Hernández[1], Demetrio Salvador Fernández Reynoso[1]*, Teresa Margarita González Martínez[1], José Donaldo Ríos Berber[1], Liborio González Hernández[2]

[1]Colegio de Postgraduados, Campus Montecillo. México.
[2]Universidad Autónoma Chapingo. México.

*Autor para correspondencia; correo-e: demetrio@colpos.mx
*Corresponding author; e-mail: demetrio@colpos.mx

Abstract

This research focuses on the calibration of an electronic monitoring system to evaluate the distribution of precipitation in two tree species: stemflow, throughfall and soil moisture. This system, focused on the application of the Arduino platform that incorporates water collection equipment, tipping buckets and humidity sensors, offers an accurate and low-cost methodology for detailed analysis of rain partitioning. This type of analysis is a critical aspect to understand the impact of vegetation covers on hydrological cycles. The lack of accessible and efficient monitoring methods has hindered a better understanding of rainfall partitioning in forest ecosystems. Calibration of tipping buckets, used to determine rainfall partitioning, have shown exceptional performance under low rainfall conditions (R^2=0.9556 to R^2=0.9878), as have soil moisture sensors. The analysis of the data collected from the tipping buckets showed a high Coefficient of determination between stemflow and direct precipitation, throughfall and direct precipitation (R^2>0.8345 and R^2>0.7723, respectively). For the moisture sensors, R^2>0.5377 was obtained in the data recorded in the field. The results obtained help a better analysis of the hydrological cycle between different tree species.

Key words: Stemflow, throughfall, forest hydrology, soil moisture, environmental monitoring, sensors.

Resumen

Esta investigación se centra en la calibración de un sistema de monitoreo electrónico para evaluar la distribución de la precipitación en dos especies arbóreas: flujo del dosel, flujo caulinar y humedad en el suelo. El sistema, centrado en la aplicación de la plataforma *Arduino*, incorpora equipos de recolección de agua, balancines y sensores de humedad; ofrece una metodología precisa y de bajo costo para el análisis detallado de la partición de la lluvia. Dicho tipo de análisis es un aspecto crítico para conocer el impacto de las cubiertas vegetales en los ciclos hidrológicos. La falta de métodos de monitoreo accesibles y eficientes han obstaculizado una mejor comprensión de la partición de la lluvia en los ecosistemas forestales. La calibración de balancines, utilizados para determinar la partición de lluvias, ha tenido un desempeño excepcional bajo condiciones de baja

precipitación (R^2=0.9556 a R^2=0.9878), al igual que los sensores de humedad del suelo. El análisis de los datos recolectados de los balancines mostró un alto coeficiente de determinación entre flujo caulinar y precipitación directa, flujo de dosel y precipitación directa (R^2>0.8345 y R^2>0.7723, respectivamente). Para los sensores de humedad se obtuvo un R^2>0.5377 en los datos registrados en campo. Los resultados obtenidos ayudan a un mejor análisis del ciclo hidrológico entre diferentes especies arbóreas.

Palabras clave: Flujo caulinar, flujo de dosel, hidrología forestal, humedad del suelo, monitoreo ambiental, sensores.

Introduction

Rainfall partitioning refers to the way in which different tree species intercept, store and redistribute precipitation, which has significant implications for ground-level water fluxes and nutrient cycling (Van Stan *et al.*, 2011). Thus, forests represent an important interface between the atmosphere and the land surface, which can interact, alter, influence and modify the interception of rainwater by the tree canopy (Munishi and Shear, 2005; Frost and Levia, 2014).

Methods to study rainfall partitioning across tree species include direct measurements (totalizing gauges), computational modeling (geostatistical analysis with meteorological information), and laboratory experiments (Keim *et al.*, 2005). These methods provide detailed information on how different tree species intercept, store and redistribute rainfall, and how these processes are influenced by factors such as tree morphology, foliage density and environmental conditions (Levia and Frost, 2006; Zimmermann *et al.*, 2007). To monitor hydrological impacts, direct measurements that reflect environmental conditions are needed (Manfroi *et al.*, 2004; Zimmermann *et al.*, 2006). Arduino-based data loggers can considerably extend hydrological monitoring networks, offering low-cost and easy-to-deploy solutions.

However, the application is still in the early stages of development, although studies have been carried out exploring its potential in hydrological monitoring

(Rahman *et al.*, 2015; Kalashnikov *et al.*, 2017), and in environmental monitoring in general (Bitella *et al.*, 2014; Divani *et al.*, 2016).

In this context, the objective of this research was to develop and calibrate an Arduino-based monitoring system to compare rainfall partitioning between *Prunus capuli* Cav. (*capulín*) and *Casuarina equisetifolia* L. (*casuarina*) through monitoring canopy and canopy flow, as well as soil moisture.

Materials and Methods

Study area

Figure 1 shows the study area where four study sites were instrumented (98°56'-98°54' W y 19°27'-19°28' N), located with a Garmin® GPS device (Etrex 22x). The area is located in a transition between a semi-dry and sub-humid temperate climate, with 700 mm average annual precipitation (García, 1968). The soils are deep (>2.0 m), with 1 to 2 % slopes, medium texture and moderate water retention capacity (Jasso and Pimentel, 1985). To evaluate the rain partition, two *Prunus capuli* (*capulín*) and *Casuarina equisetifolia* (*casuarina*) specimens were selected through transects, with safe access to the 120 V alternating current electrical energy network to power the dataloggers.
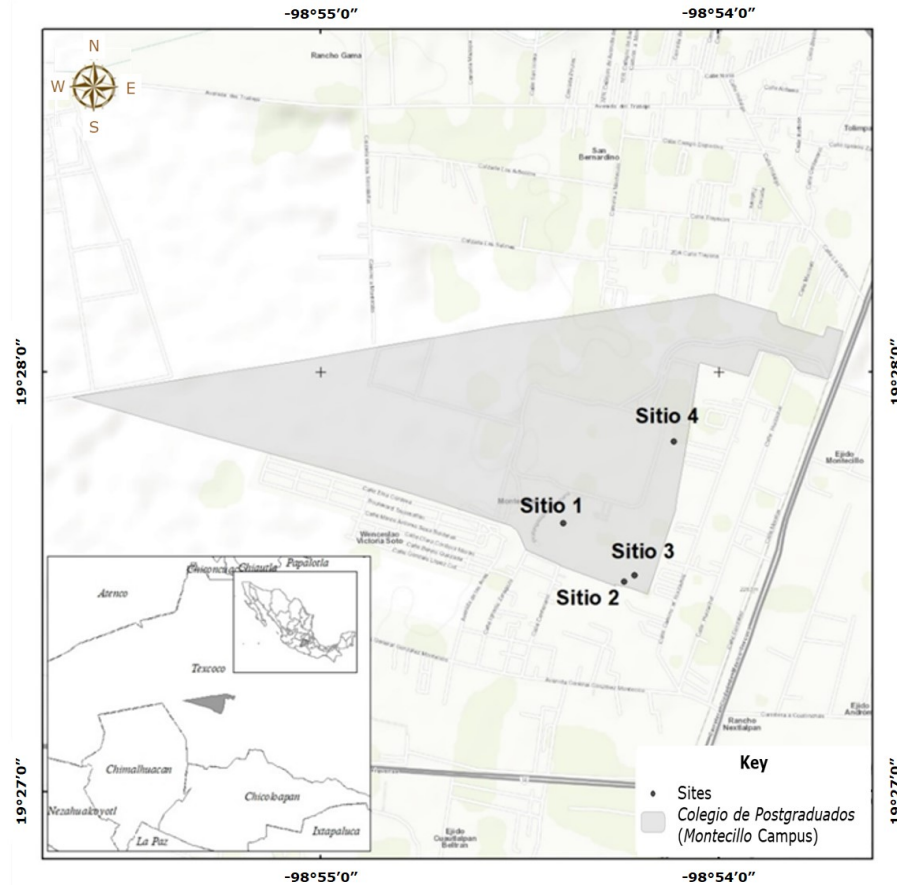
Sitio 1 = Site 1; *Sitio* 2 = Site 2; *Sitio* 3 = Site 3; *Sitio* 4 = Site 4.

Figure 1. Location of the study area and plots.

For the recording of variables, four dataloggers were designed (one per site), to which a soil humidity sensor and three tipping buckets with magnetic reed switches were installed to estimate the canopy and canopy flow, and direct precipitation (dos Santos *et al.*, 2020). The components of each datalogger include an Arduino® Mega 2560 board, a real-time clock chip (DS3231 RTC Module), a micro SD external memory reader module (for Arduino) and an OLED screen (SSD1306 128×64). These elements were mounted on a printed circuit board (custom PCB), designed through PCB Wizard and assembled. The Arduino was programmed in the open source Arduino software IDE (C/C++) (Arduino, 2021) via a USB cable to query sensor

readings every 10 minutes and record the data to an SD card. The power supply was through the electric network.

Calibration of the tipping buckets in the laboratory

The tipping buckets pluviometer (own design) was used to measure precipitation in real time, with Arduino technology, by means of a magnetic switch that is activated by tilting the PVC tipping bucket (Figure 2) when it accumulates 18 cm^3 of water (Strangeways, 2007; Santana *et al.*, 2015).
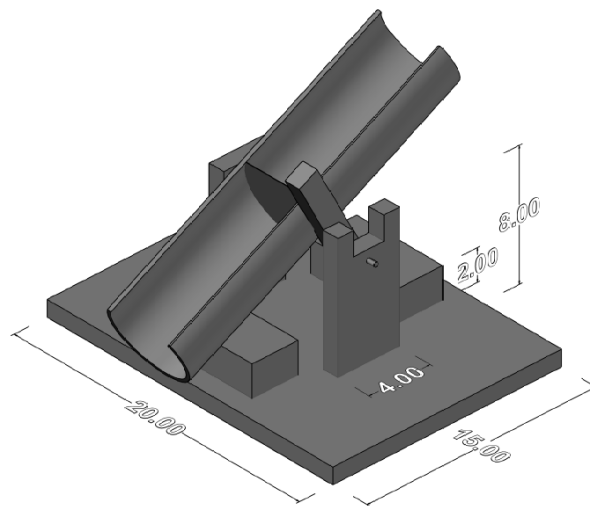

Figure 2. Diagram of the tipping bucket made of PVC.

In the Rain Simulator Laboratory of the *Colegio de Postgraduados* (*Montecillo* Campus) (Figure 3), the overturning volume recorded by the magnetic sensor was

calibrated. Under field conditions, the accuracy of the tipping buckets was compared with measurements from totalizing rain pluviometers that served as controls to validate the accuracy of the records in real conditions (Krishnamurthi *et al.*, 2015).

Figure 3. Calibration of pluviometers with the rain simulator.

Instantaneous precipitation was measured by recording the oscillations of the tipping buckets through a magnet and magnetic reed switch. The sensor, housed in a glass tube, recorded the voltage generated when an electrical circuit was closed, information that was transmitted to the datalogger. In total, for the four sites, 12 tipping buckets were used to measure stemflow, canopy flow and direct precipitation.

The calibration of the tipping buckets was carried out based on the principles of dynamic calibration (Edwards *et al.*, 1974; Lee *et al.*, 1996), that is, the values of the rain simulator were compared with the measurements of the tipping bucket, for four rain intensities (0.33, 0.83, 1.08 and 1.62 mm min^{-1}, based on the methodology of Morin *et al.* [1967]) and ten repetitions of each one. A 20 cm^3 overturning volume per bucket and a catchment area of 660 cm^2 were considered.

With the obtained results, calibration curves were prepared, and the rain intensity rate of the simulator was compared with the rate recorded in the datalogger, in order to know the precision and reliability of the data.

The effectiveness of the calibration curve was evaluated through the Nash-Sutcliffe Efficiency (*NSE*) and *PBIAS*, as set out in Equation 1 and 2, respectively (Somavilla *et al.*, 2019).

$$NSE = 1 - \left(\frac{\sum_{i=1}^{n}\left(Y_1^{ad} - Y_1^{est}\right)^2}{\sum_{i=1}^{n}\left(Y_1^{ad} - Y_1^{mean}\right)^2} \right) \quad (1)$$

Where:

n = Number of evaluations

Y_1^{ad} = Added flow

Y_1^{est} = Estimated flow by the instrument

Y_1^{mean} = Mean of the added flow

$$PBIAS = \left(\frac{\sum_{i=1}^{n}\left(Y_1^{ad} - Y_1^{est}\right)}{\sum_{i=1}^{n}\left(Y_1^{ad}\right)} \right) \times 100 \quad (2)$$

Where:

Y_1^{ad} = Added flow

Y_1^{est} = Estimated flow by the instrument

Calibration of humidity sensors in the laboratory

To calibrate the capacitive soil moisture sensors, soil samples were taken at 15 cm depth with known moisture at the 4 study sites. The samples were placed in perforated jars based on the methodology of Gil-Marin *et al.* (2022). In the aforementioned laboratory, the initial weight of the samples was measured (PC 2000 Mettler® scale) and readings were taken with the capacitive sensor (Capacitive Hygrometer Module v1.2 for Arduino) (Figure 4), which works through the apparent dielectric constant of the floor.

The flasks were partially sealed to facilitate the entry of water by capillarity and were immersed in trays with distilled water at different humidity contents (10 to 80 mL). After one day, upon reaching saturation, each sample was weighed and the gravimetric humidity was measured with the sensor. The gravimetric water content was determined by the difference in weight after drying, ten times, with two replications. The sensor readings and measurements of the gravimetric soil moisture content were related, with linear regression analysis the precision of the results was determined through the Coefficient of determination (R^2) (Gil-Marin *et al.*, 2022).

Figure 4. Determination of readings with the capacitive sensor.

Soil moisture in real rain conditions

Once the capacitive soil moisture sensors were calibrated, the evaluation of soil moisture levels in the four study sites was carried out with the digital outputs recorded in the datalogger. The sensor was placed at a depth of 10 cm in order to measure moisture at the level of the roots of the trees.

Stemflow in real rain conditions

Stemflow measurement was carried out by means of a collection system installed on the tree trunks, which included a collecting ring 1 m high, fixed to the trunk to direct the water towards a flexible hose, reinforced with sisal rope and plasticine, which was discharged to a tipping bucket previously calibrated to volumetric units (Figure 5). To obtain the water depth (mm), Equation 3, proposed by Barbosa *et al.* (2016) was used.

Figure 5. Arrangement used to measure stemflow in *Prunus capuli* Cav.

$$F_c = \left(\frac{v_{pb}}{A_c} \times 1\,000\right) \times n_b \qquad (3)$$

Where:

F_c = Stemflow (mm)

v_{pb} = Average volume captured by the containers of the tipping buckets by overturning (m³)

A_c = Crown area (m²)

n_b = Number of overturns of the containers of the tipping buckets during the rain event

Throughfall in real rain conditions

To measure the water that passes through the canopy (throughfall), two triangular-shaped gutters (30 cm per side and 130 cm long) were installed below the tree canopy (Figure 6). The water depth per rain event was calculated with Equation 4 (Barbosa *et al.*, 2016).

Figure 6. Arrangement of gutters used to estimate canopy flow.

$$F_d = \frac{v_c}{A_{cc}} \times 1\,000 \qquad (4)$$

Where:

F_d = Canopy flow (mm)

v_c = Volume captured in the gutter from rain event (m^3)

A_{cc} = Gutter catchment area (m^2)

To know the instantaneous depth of water throughout the rain event, a second channel was installed that directed the flow of water to a previously calibrated tipping bucket.

In this case, the flow estimation was through the volume captured by the tipping bucket and the number of overturns using Equation 5 (Barbosa *et al.*, 2016).

$$F_{db} = \frac{(v_{pb} \times n_b)}{A_{cc}} \times 1\,000 \qquad (5)$$

Where:

F_{db} = Throughfall with tipping bucket (mm)

v_{pb} = Average volume captured by the containers of the tipping buckets per overturn (m^3)

n_b = Number of overturns of the containers of the tipping buckets during the rain event

A_{cc} = Gutter catchment area (m^2)

Direct precipitation in real rain conditions

To measure direct precipitation per site, a rain gauge composed of two overlapping plastic buckets of 29 cm in diameter and 36 cm in height was used; the bottom diameter of the acetate sheet funnel is 3 mm. One of the calibrated tipping buckets was adapted to the upper bucket and its bottom was drilled in order to capture the water poured by the tipping bucket in the lower bucket (Figure 7). With the relationship between the volume of water collected in the lower bucket and the surface of the pluviometer, the precipitation sheet was determined. The tipping

bucket precipitation sheet was obtained from the number of overturns recorded in the datalogger by using Equation 6 (Barbosa *et al.*, 2016).

Figure 7. Arrangement of rain gauges used to measure precipitation.

$$P_{d2} = \frac{(v_{pb} \times n_b)}{A_{pl}} \times 1\,000 \qquad (6)$$

Where:

P_{d2} = Direct precipitation with the tipping bucket (mm)

v_{pb} = Captured volume with the tipping bucket per overturn (m³)

n_b = Number of overturns of the tipping bucket during the rain event

A_{pl} = Catchment area from the pluviometer (m²)

The amount of water captured, in volumetric units, is determined based on Equation 7 (Barbosa *et al.*, 2016):

$$P_{d1} = \frac{v_{pl}}{A_{pl}} \times 1\,000 \qquad (7)$$

Where:

P_{d1} = Direct precipitation (mm)

v_{pl} = Captured volume with the pluviometer per rain event (m^3)

A_{pl} = Catchment area from the pluviometer (m^2)

Rainfall records were made between July 16th, 2022 and October 18th, 2022, a period that allowed rain data to be collected under a wide range of wind conditions and rain intensity.

Results and Discussion

Calibration of tipping buckets in the laboratory (rain simulator)

The twelve tipping buckets used in the present study were calibrated in a rain simulator with ten repetitions per intensity, which gave a total of 480 events. Actual precipitation was compared to the tipping buckets readings to calculate coefficients of determination (Hudson, 1993). The results between the tipping buckets measurements and the actual values showed a high correlation (R^2=0.9556 to

R^2=0.9878) (Table 1), and confirmed the effectiveness of the Arduino-controlled tipping buckets for monitoring rain partitioning in tree covers.

Table 1. Linear adjustment models for tipping buckets arm calibration.

Tipping bucket	Equation	R^2	RMSE	NSE	PBIAS
1	$y = 0.9556x$	0.9869	0.069	0.9780	3.83
2	$y = 0.9572x$	0.9839	0.071	0.9763	3.52
3	$y = 0.9878x$	0.9909	0.045	0.9907	0.67
4	$y = 0.9831x$	0.9830	0.060	0.9830	0.83
5	$y = 0.9741x$	0.9823	0.065	0.9806	1.76
6	$y = 0.982x$	0.9842	0.058	0.9844	0.62
7	$y = 0.9631x$	0.9869	0.063	0.9814	2.79
8	$y = 0.9684x$	0.9909	0.054	0.9864	2.69
9	$y = 0.9676x$	0.9883	0.059	0.9839	2.59
10	$y = 0.9872x$	0.9847	0.057	0.9849	0.56
11	$y = 0.9668x$	0.9792	0.071	0.9764	2.12
12	$y = 0.9747x$	0.9894	0.053	0.9864	1.85

The results of the study demonstrate that Arduino-controlled tipping buckets offer high correlations in measuring rainfall at different precipitation intensities (Fankhauser, 1997; Habib *et al.*, 2008; Shedekar *et al.*, 2016; Segovia-Cardozo *et al.*, 2023). These correlations consider the influence of factors such as the structure of the pluviometer and its configuration on the measurements (Fankhauser, 1997; Shedekar *et al.*, 2009).

A significant variation in the coefficients of determination was observed between the tipping buckets, indicating that specific construction and assembly conditions can affect performance, which can be corroborated by the *PBIAS* coefficients (0.56 to 3.83). Despite these variations, the tipping buckets proved to be robust and reliable (*NSE*=0.9763 to *NSE*=0.9907), confirming their usefulness even in the face of variations in construction conditions and different precipitation intensities (Chrit, 2022).

These findings underscore the potential of Arduino-controlled tipping buckets as valuable tools for precipitation research and monitoring.

Calibration of the moisture sensor in the laboratory

In the calibration of the humidity sensors, for the soil samples from the four sampling sites, the different sensor readings were related to the percentage of gravimetric moisture of the soil samples.

The calibration curves were fitted to a logarithmic model with high coefficients of determination: 0.9198, 0.9192, 0.9849 and 0.9264 for sites 1, 2, 3 and 4, respectively (Table 2). The values obtained in the present investigation are similar to those reported by Placidi *et al.* (2020), who adjusted their calibration curve to a second-order function and with a Coefficient of determination of 0.945.

Table 2. Calibration adjustment models of moisture sensors.

Moisture sensor	Equation	R^2
Site 1 (*Casuarina equisetifolia* L.)	$y = -56.52 ln(x) + 374.84$	0.9198
Site 2 (*Prunus capuli* Cav.)	$y = -55.87 ln(x) + 348.02$	0.9192

Site 3 (*Prunus capuli* Cav.)	$y = -62.82ln(x) + 379.39$	0.9849
Site 4 (*Casuarina equisetifolia* L.)	$y = -101.6ln(x) + 630.05$	0.9264

This analysis reveals that Arduino moisture sensors are a reliable tool for accurately measuring soil moisture, despite variations in analysis sites. The high correlation values indicate that measurements made with humidity sensors achieve high precision and consistency (Lloyd and Marques, 1988; Levia and Frost, 2006).

Evaluation of tipping buckets in field conditions

In the evaluation of the tipping buckets, previously calibrated in the laboratory, they continued to register a high positive linear correlation, under field conditions, between the canopy flow (throughfall) with tipping buckets and the volume of control water. The results gathered in Table 3 confirm the accuracy and effectiveness of the tipping buckets in measuring throughfall and direct rainfall of the four sites under study.

Table 3. Tipping bucket adjustment models under throughfall and direct rainfall conditions (tipping bucket *vs.* control).

Site	Type of flow	Species	Equation	R^2
1	Canopy	*Casuarina equisetifolia* L.	$y = 1.1031x$	0.9783
2	Canopy	*Prunus capuli* Cav.	$y = 1.1343x$	0.9755

3	Canopy	*Prunus capuli* Cav.	$y = 1.0841x$	0.9762
4	Canopy	*Casuarina equisetifolia* L.	$y = 1.0485x$	0.9588
1	Direct rainfall	*Casuarina equisetifolia* L.	$y = 0.9670x$	0.9827
2	Direct rainfall	*Prunus capuli* Cav.	$y = 1.0379x$	0.9667
3	Direct rainfall	*Prunus capuli* Cav.	$y = 1.0262x$	0.9595
4	Direct rainfall	*Casuarina equisetifolia* L.	$y = 1.0591x$	0.9727

The strong correlations across all sites (Table 3) suggest that tipping buckets are an effective tool for measuring canopy flow in different tree cover types, which is crucial for understanding precipitation partitioning in such species (Staelens *et al.*, 2006). Likewise, they turn out to be effective instruments for measuring precipitation and an alternative in meteorological, climatic studies and those that evaluate the hydrological impact of the forest characteristics of the trees (density, arrangement, texture and shape of the leaves) on the runoff and infiltration of rain (Levia and Frost, 2006).

Partitioning of direct rainfall (stemflow and throughfall) and soil moisture

The analysis of the data collected from the tipping buckets showed a high positive correlation between the stemflow and direct precipitation (Figure 8, example corresponding to *Casuarina equisetofolia* from Site 1), where the correlations were 0.8345, 0.9163, 0.8471 and 0.9087 for the sites 1, 2, 3 and 4, respectively (Table 4). This means that as direct rainfall increases, so does stemflow.
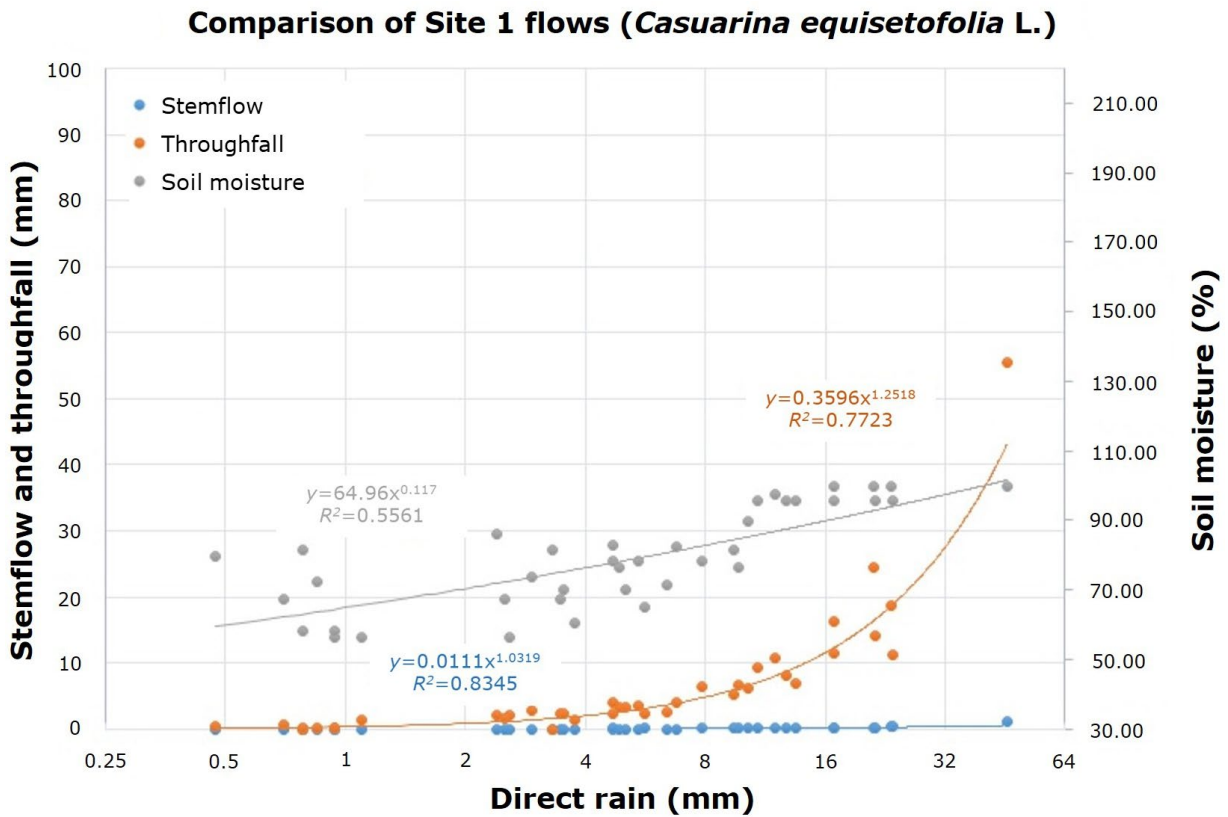
Figure 8. Relationship between direct precipitation and streamflow from Site 1.

Table 4. Adjustment models between direct precipitation *vs.* stemflow, throughfall and soil moisture.

Site	Type of measurement	Species	Equation	R^2
1	Stemflow	*Casuarina equisetifolia* L.	$y = 0.0111x^{1.0319}$	0.8345
2	Stemflow	*Prunus capuli* Cav.	$y = 0.0047x^{1.1992}$	0.9163
3	Stemflow	*Prunus capuli* Cav.	$y = 0.0072x^{0.9379}$	0.8471
4	Stemflow	*Casuarina equisetifolia* L.	$y = 0.0073x^{1.1828}$	0.9087
1	Throughfall	*Casuarina equisetifolia* L.	$y = 0.3596x^{1.2518}$	0.7723
2	Throughfall	*Prunus capuli* Cav.	$y = 0.3451x^{1.2286}$	0.9155

3	Throughfall	*Prunus capuli* Cav.	$y = 0.3881x^{1.1908}$	0.9177
4	Throughfall	*Casuarina equisetifolia* L.	$y = 0.2889x^{1.3536}$	0.8332
1	Soil moisture	*Casuarina equisetifolia* L.	$y = 64.96x^{0.117}$	0.5561
2	Soil moisture	*Prunus capuli* Cav.	$y = 44.683x^{0.175}$	0.5416
3	Soil moisture	*Prunus capuli* Cav.	$y = 35.614x^{0.2319}$	0.5377
4	Soil moisture	*Casuarina equisetifolia* L.	$y = 41.158x^{0.2328}$	0.5479

In Figure 8 it can be seen that this (stemflow) represents around 3 % of the precipitation, a pattern that is repeated in the other sites, similar to what was recorded by Gómez-Tagle *et al.* (2015) who determined a cortical runoff proportion of 2.4 % for a secondary pine-oak forest in the Northeast of the state of *Michoacán*.

In spite of showing greater variability, the correlation between direct precipitation and canopy flux is high (Table 4): Site 1 (0.7723), Site 2 (0.9155), Site 3 (0.9177) and Site 4 (0.8332), indicating the good performance of the tipping bucket in the field.

The relationships between direct rainfall and soil moisture had similar coefficients of determination (Table 4) (0.5561, 0.5416, 0.5377 and 0.5479 for sites 1, 2, 3 and 4, respectively), indicating an increase in relatively low between rain events, as they are very intense. The coefficients of determination obtained are similar to those calculated by Cheng *et al.* (2020), who obtained an $R^2=0.3518$ for abandoned crops and an $R^2=0.5015$ for shrublands.

The comparison of the costs of dataloggers with the prices of analogous measuring instruments is USD \$1 396 (Table 5).

Table 5. Price of the designed equipment *vs.* those available on the market (prices in US dollars).

Datalogger and designed sensors	Cost per unit	Datalogger and commercial sensors	Cost per unit

Datalogger (Including Arduino board, memory module, reed switch and real time clock)	$46.00	HOBO® RX3000 Remote Monitoring StationData Logger	$1 180.00
Tipping bucket (own design), channel and sensor	$58.00	Davis Rain Sensor (Pluviometer)	$135.00
Capacitive soil moisture sensor	$5.00	The Decagon ECH2O (Soil moisture sensor)	$190.00
Total	$109.00	Total	$1 505.00

Conclusions

This study highlighted the efficiency of tipping buckets designed with Arduino to measure precipitation under controlled conditions, demonstrating their adaptability to different rain conditions. The affordability, feasibility and accuracy of the tipping buckets and humidity sensor make them viable for remote locations in disciplines such as hydrology, climatology and agriculture.

Using Arduino as a control and data collection platform opens the door to a wide range of scientific applications. Future research could explore the integration of Arduino into other measurement instruments and its comparison with scientifically proven instruments, such as temperature and humidity sensors, for a more comprehensive analysis of climate and its impacts in various fields.

Acknowledgements

Conflict of interest

The authors state no conflict of interest.

Contribution by author

Daniel García-Hernández: field-data collection and writing of the manuscript; Demetrio Salvador Fernández Reynoso: review of the methodology and the manuscript; Teresa Margarita González Martínez: review of the methodology; José Donaldo Ríos Berber and Liborio González Hernández: review of the manuscript.

References

Arduino. 2021. Arduino IDE (Versión 1.8.16). Ivrea, TO, Italia. Arduino. https://www.arduino.cc/en/software. (19 de noviembre de 2023).

Barbosa M., F., D. S. Fernández R., E. Rubio G., I. Sánchez C. y J. R. Contreras H. 2016. Dinámica del agua de lluvia en árboles de selva baja caducifolia. Revista Mexicana de Ciencias Agrícolas 7(5):1179-1188. Doi: 10.29312/remexca.v7i5.241.

Bitella, G., R. Rossi, R. Bochicchio, M. Perniola and M. Amato. 2014. A novel low-cost open-hardware platform for monitoring soil water content and multiple soil-air-vegetation parameters. Sensors 14(10):19639-19659. Doi: 10.3390/s141019639.

Cheng, R.-R., Q.-W. Chen, J.-G. Zhang, W.-Y. Shi, G. Li and S. Du. 2020. Soil moisture variations in response to precipitation in different vegetation types: A multi-year study in the loess hilly region in China. Ecohydrology 13(3):e2196. Doi: 10.1002/eco.2196.

Chrit, M. 2022. *Ensemble calibration and uncertainty quantification of precipitation forecasts for a risk-based UAS Navigation*. https://d197for5662m48.cloudfront.net/documents/publicationstatus/117374/preprint_pdf/eb72b3111da15500d2bee67c85facf6d.pdf. (25 de noviembre de 2023).

Divani, D., P. Patil and S. K. Punjabi. 2016. Automated plant watering system. *In*: Institute of Electrical and Electronic Engineers (IEEE) (Edit.). 2016 International Conference on Computation of Power, Energy Information and Communication (ICCPEIC). IEEE. Melmaruvathur, TN, India. pp. 180-182.

dos Santos, B. C., M. S. Duarte S., D. N. Buarque P., P. H de Souza and A. R. Bruno T. 2020. Low cost rain gauge prototype for studies and monitoring of precipitation in anthropized watersheds. Cuaderno de Geografía 30(63):923-935. Doi: 10.5752/p.2318-2962.2019v30n63p923.

Edwards, I. J., W. D. Jackon and P. M. Fleming. 1974. Tipping bucket gauges for measuring runoff from experimental plots. Agricultural Meteorology 13(2):189-201. Doi: 10.1016/0002-1571(74)90046-6.

Fankhauser, R. 1997. Measurement properties of tipping bucket rain gauges and their influence on urban runoff simulation. Water Science & Technology 36(8-9):7-12. Doi: 10.2166/wst.1997.0636.

Frost, E. E. and D. F. Levia. 2014. Hydrologic variation of stemflow yield across co-occurring dominant canopy trees of varying mortality. Ecohydrology 7(2):760-770. Doi: 10.1002/eco.1397.

García, E. 1968. Los climas del Valle de México. Colegio de Postgraduados. Texcoco, Edo. Méx., México. 57 p.

Gil-Marin, J., M. Cordova-Rodriguez y A. Zermeño-Gonzalez. 2022. Calibración de sensores de reflectometría de dominio temporal en suelos ultisoles de sabana. Anales Científicos 83(1):57-66. Doi: 10.21704/ac.v83i1.1884.

Gómez-Tagle C., A., A. F. Gómez-Tagle R., J. A. Ávila O. y L. A. Bruijnzeel. 2015. Partición de la precipitación en un bosque tropical montano de pino-encino en el centro de México. Bosque 36(3):505-518. Doi: 10.4067/S0717-92002015000300017.

Habib, E. H., E. A. Meselhe and A. V. Aduvala. 2008. Effect of local errors of tipping-bucket rain gauges on rainfall-runoff simulations. Journal of Hydrologic Engineering 13(6):488-496. Doi: 10.1061/(ASCE)1084-0699(2008)13:6(488).

Hudson, N. 1993. Field measurement of soil erosion and runoff. Food and Agriculture Organization of the United Nations (FAO). Rome, RM, Italy. 139 p. https://www.fao.org/4/T0848E/T0848E00.htm. (19 de noviembre de 2023).

Jasso M., J. y L. Pimentel B. 1985. Establecimiento de áreas verdes en el predio Montecillo aledaño a Chapingo. *In:* Secretaría de Agricultura y Recursos Hidráulicos (SARH) (Edit.). III Reunión Nacional sobre Plantaciones Forestales. Instituto Nacional de Investigaciones Forestales, Agrícolas y Pecuarias (INIFAP). México, D. F., México. pp. 606-640.

Kalashnikov, A., H. Zhang, J. Jennings and M. M. Abramriuk. 2017. Remote laboratory: using Internet-of-Things (IoT) for E-learning. *In*: Faculty of Electronics and Information Technologies (Edit.). The Vth International Conference «Advanced Information Systems and Technologies, AIST 2017». Ukrainian Federation of Informatics. Sumy, BM, Ukraine. pp. 43-46.

Keim, R. F., A. E. Skaugset and M. Weiler. 2005. Temporal persistence of spatial patterns in throughfall. Journal of Hydrology 314(1-4):263-274. Doi: 10.1016/j.jhydrol.2005.03.021.

Krishnamurthi, K., S. Thapa, L. Kothari and A. Prakash. 2015. Arduino Based Weather Monitoring System. International Journal of Engineering Research and General Science 3(2):452-458. https://pnrsolution.org/Datacenter/Vol3/Issue2/64.pdf. (19 de noviembre de 2023).

Lee, D. W., K. Baskaran, M. Mansor, H. Mohamad and S. K. Yap. 1996. Irradiance and spectral quality affect Asian tropical rain forest tree seedling development. Ecology 77(2):568-580. Doi: 10.2307/2265631.

Levia, D. F. and E. E. Frost. 2006. Variability of throughfall volume and solute inputs in wooded ecosystems. Progress in Physical Geography: Earth and Environment 30(5):605-632. Doi: 10.1177/0309133306071145.

Lloyd, C. R. and A. de O Marques F. 1988. Spatial variability of throughfall and stemflow measurements in Amazonian rainforest. Agricultural and Forest Meteorology 42(1):63-73. Doi: 10.1016/0168-1923(88)90067-6.

Manfroi, O. J., K. Koichiro, T. Nobuaki, S. Masakazu, … and L. Chong. 2004. The stemflow of trees in a Bornean lowland tropical forest. Hydrological Process 18(13):2455-2474. Doi: https://doi.org/10.1002/hyp.1474.

Morin, J., D. Goldberg and I. Seginer. 1967. A rainfall simulator with rotating disk. Transactions of the American Society of Agricultural Engineers 10:74-77. Doi: 10.13031/2013.39599.

Munishi, P. K. T. and T. H. Shear. 2005. Rainfall interception and partitioning in afromontane rain forests of the eastern arc mountains, Tanzania: implications for water conservation. Journal of Tropical Forest Science 17(3):355-365. https://jtfs.frim.gov.my/jtfs/article/view/1045/881. (19 de noviembre de 2023).

Placidi, P., L. Gasperini, A. Grassi, M. Cecconi and A. Scorzoni. 2020. Characterization of low-cost capacitive soil moisture sensors for IoT networks. Sensors 20(12):3585. Doi: 10.3390/s20123585.

Rahman, M., N. E-Jannat, O. Islam and S. Salakin. 2015. Arduino and GSM based smart energy meter for advanced metering and billing system. *In*: Institute of

Electrical and Electronic Engineers (IEEE) (Edit.). 2015 International Conference on Electrical Engineering and Information Communication Technology (ICEEICT). IEEE. Savar, D, Bangladés. pp. 1-6.

Santana, M. A. A., P. L. O. Guimarães, L. G. Lanza and E. Vuerich. 2015. Metrological analysis of a gravimetric calibration system for tipping-bucket rain gauges. Meteorological Applications 22(S1):879-885. Doi: 10.1002/met.1540.

Segovia-Cardozo, D. A., C. Bernal-Basurco and L. Rodríguez-Sinobas. 2023. Tipping bucket rain gauges in hydrological research: Summary on measurement uncertainties, calibration, and error reduction strategies. Sensors 23(12):5385. Doi: 10.3390/s23125385.

Shedekar, V. S., K. W. King, L. C. Brown, N. R. Fausey, M. Heckel and R. D. Harmel. 2009. Measurement errors in tipping bucket rain gauges under different rainfall intensities and their implication to hydrologic models. *In*: American Society of Agriculture and Biological Engineers (ASABE) (Edit.). 2009 ASABE Annual International Meeting Sponsored. ASABE. Reno, NV, United States of America. pp. 1-9.

Shedekar, V. S., K. W. King, N. R. Fausey, A. B. O. Soboyejo, R. D. Harmel and L. C. Brown. 2016. Assessment of measurement errors and dynamic calibration methods for three different tipping bucket rain gauges. Atmospheric Research 178-179:445-458. Doi: 10.1016/j.atmosres.2016.04.016.

Somavilla, A., P. I. Gubiani and A. L. Zwirtz. 2019. Tipping bucket prototype for automatic quantification of surface runoff rate in plots. Revista Brasileira de Ciência do Solo 43:1-7. Doi: 10.1590/18069657rbcs20180096.

Staelens, J., A. De Schrijver, K. Verheyen and N. E. C. Verhoest. 2006. Spatial variability and temporal stability of throughfall water under a dominant beech (*Fagus sylvatica* L.) tree in relationship to canopy cover. Journal of Hydrology 330(3-4):651-662. Doi: 10.1016/j.jhydrol.2006.04.032.

Strangeways, I. 2007. Precipitation: Theory, measurement and distribution. Cambridge University Press. Cambridge, Cambs., United Kingdom. 290 p.

Van Stan II, J. T., C. M. Siegert, D. F. Levia and C. E. Scheick. 2011. Effects of wind-driven rainfall on stemflow generation between codominant tree species with differing crown characteristics. Agricultural and Forest Meteorology 151(9):1277-1286. Doi: 10.1016/j.agrformet.2011.05.008.

Zimmermann, B., H. Elsenbeer and J. M. De Moraes. 2006. The influence of land-use changes on soil hydraulic properties: Implications for runoff generation. Forest ecology and Management 222(1-3):29-38. Doi: 10.1016/j.foreco.2005.10.070.

Zimmermann, A., W. Wilcke and H. Elsenbeer. 2007. Spatial and temporal patterns of throughfall quantity and quality in a tropical montane forest in Ecuador. Journal of Hydrology 343(1-2):80-96. Doi: 10.1016/j.jhydrol.2007.06.012.